Journal of Bio & Geo Material and Energy (BiGME)
Volume 6 No. 1, February 2026
P-ISSN: 2808-1560 E-ISSN: 2808-1404

Influence of Mass Variation of Green-Synthesized $CoFe_2O_4$/Cdots Catalyst on the Photocatalytic Degradation of Methylene Blue Through Initial Adsorption Mechanism

Aldwin Zalukhu[1], Frastica Deswardani[1*], Edi Suharyadi[2], RantiWidia Utami[2], Nurul Imani Istiqomah[2], Larrisa Jestha Mahardhika[2], Siti Fatimah Azzahro[2], Dapfa Farrizo Altop[1], Nada Oktaviani[1]

[1]Department of Physics, Faculty Science and Technology, University of Jambi
[2]Department of Physics, Faculty of Mathematics and Natural Sciences, University of Gadjah Mada

Email: frastica.deswardani@unja.ac.id

Article Info

Submited: November 2025
Revised: December 2025
Accepted: January 2026
Published: February 2026

***Abstract* :**
This study aimed to synthesize and evaluate the photocatalytic performance of $CoFe_2O_4$/Cdots nanocomposites prepared via green synthesis method using Moringa oleifera leaf extract and watermelon rind waste as an eco friendly precursors. The synthesis involved a co-precipitation process for $CoFe_2O_4$ formation and a hydrothermal route to produced Cdots, followed by composite fabrication. The materials were characterized using XRD, UV-Vis Spectrophotometer, and VSM analyses to determine their crystalline structure, optical, and magnetic properties. The results showed that the incorporation of Cdots increased the optical band gap (3.15 eV) compared to pure $CoFe_2O_4$ (2.64 eV) and improved soft magnetic behavior. Photocatalytic tests under UV irradiation using Methylene Blue as a model pollutant revealed a degradation efficiency of 91.9% for $CoFe_2O_4$/Cdots at an optimum catalyst mass of 0.07 gr, significantly higher than 60,8% achieved by pure $CoFe_2O_4$. The enhanced performance is attributed to the synergistic interaction between $CoFe_2O_4$ and Cdots, which promotes charge separation, initial adsorption, and reactive radical generation. These findings indicate that the $CoFe_2O_4$/Cdots nanocomposite is a promising eco-friendly photocatalyst for wastewater treatment applications.

Keywords: Adsorption; $CoFe_2O_4$/CdotS; Methylene Blue degradation; photocatalyst

1. Introduction

The issue of water pollution by synthetic dyes remains a pressing environmental issue, particularly in countries with high textile and laboratory activity. Indonesia has a large textile and batik industry, resulting in colored wastewater that requires special treatment. Batik waste contains dyes and chemicals that can pollute rivers and the surrounding environment (Hannan et al., 2024). One frequently used synthetic dye is Methylene Blue (MB), which is difficult to decompose, reduces light penetration in water, disrupts photosynthesis by biota, and is potentially toxic, endangering ecosystems and human health (Oladoye et al., 2022). Due to its persistence, MB is often detected after industrial production and washing processes, requiring treatment that goes beyond simply removing the pollutant but also thoroughly degrading it to a safer environment. Various methods for degrading MB waste have been implemented, including coagulation/flocculation, membrane filtration, adsorption, electrocoagulation, vacuum membrane distillation, nanofiltration, ultrafiltration, and advanced oxidation processes (AOPs). While each of these methods is effective to some extent, they have significant limitations, including the need for additional chemicals, high operational costs, membrane fouling issues, and the formation of difficult-to-manage secondary sludge or residue (Lucas et al., 2025). Despite these limitations, one promising method for Methylene Blue (MB) degradation is photocatalyst. This method is considered more environmental friendly than conventional techniques such as coagulation and chemical oxidation because it produces no additional hazardous waste and utilizes light energy, either from sunlight or artificial sources, to activate semiconductor materials as catalysts (Salehi et al., 2024).

One semiconductor frequently used as a catalyst in photocatalysis is Cobalt Ferrite ($CoFe_2O_4$). This material belongs to the spinel ferrite group with a cubic crystal structure, is ferrimagnetic, and has a narrow

semiconductor band gap, making it possible to use it for visible light absorption (Kareem et al., 2022). The advantages of $CoFe_2O_4$ over other metal oxides are its chemical stability, magnetic properties that facilitate post-reaction separation, and its relatively high organic pollutant degradation capacity (Kunarti et al., 2025). However, the photocatalytic performance of pure $CoFe_2O_4$ still has significant limitations, primarily due to the rapid recombination of electron-hole pairs (e^-/h^+) formed when this material is excited by light (Wang & Bin, 2019). This high recombination process results in only a small fraction of electrons and holes actually participating in the photocatalytic reaction, resulting in low degradation efficiency of organic dyes such as MB. Therefore, a material modification strategy is needed to significantly improve photocatalytic performance.

One promising approach is the formation of nanocomposites using Carbon Dots (Cdots). Cdots are nanoscale carbon materials (<10 nm) that exhibit distinct properties compared to conventional carbon materials (Annamalai et al., 2025). Cdots are capable of absorbing a broader spectrum of light, including visible light, thus expanding the adsorption spectrum of photocatalysts (Wang & Bin, 2019). Furthermore, to create photocatalyst materials that are not only efficient but also environmentally friendly, a synthesis method that prioritizes the use of natural, non-toxic materials and produces minimal waste is required. The Green Synthesis method meets these criteria by relying on plant extracts or biomass as reducing and stabilizing agents in the nanomaterial formation process. This approach is considered more sustainable than conventional methods, which generally use hazardous chemicals and produce toxic waste. Green Synthesis not only reduces environmental impact but also produces materials with good optical properties, morphology, and photocatalytic activity due to the presence of bioactive compounds from biological agents that play a role in the nanoparticle formation process (Vijayaram et al., 2024).

$CoFe_2O_4$ used as a photocatalyst material has been widely studied, various studies have shown that $CoFe_2O_4$-based nanocomposites have high prospects in photocatalysis applications (Lu et al., 2019). Although it has been widely developed, studies on the combination of $CoFe_2O_4$ with Cdot are still very limited, even though this combination has great potential to increase photocatalytic activity due to the nature of Cdot which has photoluminescence, a large surface area, and the ability as an electron acceptor that can reduce the recombination rate of electron-hole pairs (e^-/h^+) in photocatalysts (Maddu et al., 2021). Previous studies such as those conducted by (Wang & Bin, 2019) proved that the addition of Cdot to $CoFe_2O_4$ can increase photocatalytic activity in the degradation of Methylene Blue, but the study was still limited to certain conditions and did not systematically evaluate the effect of variations in catalyst mass on degradation efficiency. Similar findings were also seen in the study of (Ahmadian et al., 2017), where the primary focus of research is on analyzing structural properties, morphology, and charge transfer mechanisms. Critical operational aspects such as the influence of catalyst quantity have not been widely studied, even though catalyst mass is a crucial parameter in the photocatalysis process. Excessive mass can cause shading and particle agglomeration, while too little mass does not provide enough active sites to support optimal degradation (Wang & Bin, 2019).

Furthermore, most previous studies still use conventional synthesis methods based on inorganic chemicals. While these methods are effective in producing materials with good structure, their drawbacks lie in the use of toxic chemicals that potentially generate hazardous waste and do not support sustainability principles (Hassaan et al., 2023). On the other hand, green synthesis approaches are gaining attention because they utilize biomass, plant extracts, or biological agents as reducing agents and stabilizers for nanoparticles. However, research specifically combining green synthesis for the synthesis of $CoFe_2O_4$ and Cdot, and evaluating the effect of varying catalyst mass on photocatalytic performance, is still rarely reported.

This research is novel in several important aspects. First, the application of a plant based green synthesis method to the synthesis of $CoFe_2O_4$/Cdot nanocomposites produces a more environmentally friendly, affordable, and sustainable material. Second, the research focuses on evaluating the effect of varying catalyst mass on the degradation efficiency of Methylene Blue, a crucial operational aspect that has not been widely studied in previous research. Third, this research is oriented towards conditions that are more applicable to real-world problems, particularly textile and batik wastewater in Indonesia. Therefore, the results obtained not only enrich the academic literature but also have practical value in the treatment of hazardous industrial waste.

2. Research Methods

Materials

The main materials used in this study consisted of *Moringa oleifera* (Mo) powder, which acted as a natural reducing and stabilizing agent due to its rich phytochemical content such as polyphenols and flavonoids that facilitate nanoparticle formation. Watermelon rind was utilized as a carbon source for the synthesis of Cdots because it contains abundant organic compounds like cellulose and lignin that yield carbon-rich nanostructures upon hydrothermal treatment. Cobalt(II) chloride hexahydrate ($CoCl_2 \cdot 6H_2O$) and Iron(III) chloride hexahydrate ($FeCl_3 \cdot 6H_2O$) served as precursors for Co^{2+} and Fe^{3+} ions to form $CoFe_2O_4$ spinel ferrite nanoparticles. Sodium hydroxide (NaOH) functioned as a strong base to precipitate metal hydroxides, while hydrogen peroxide (H_2O_2) acted as an oxidizing agent to enhance photocatalytic degradation. Methylene Blue (MB) was used as a model dye for photocatalytic testing, and distilled water along with ethanol were employed as solvents during the synthesis and purification processes.

Synthesis

The material synthesis process was carried out using an environmental friendly green synthesis method. The first stage was the preparation of Moringa oleifera extract, where 5 g of commercially available Moringa oleifera leaf powder, purchased from CV. Timurasa Indonesia and used as received without further pretreatment, was dissolved in 60 mL of distilled water, then stirred with a magnetic stirrer at 60 °C and a speed of 600 rpm for 1 hour until homogeneous. The obtained solution was filtered using Whatman paper and the filtrate was used as a natural reducing agent. Next, the synthesis of $CoFe_2O_4$ was carried out by dissolving 1,19 gr of $CoCl_2 \cdot 6H_2O$ and 2,7 gr of $FeCl_3 \cdot 6H_2O$ each into 15 mL of distilled water, then the two solutions were mixed and stirred for 5 minutes until homogeneous. After that, Moringa oleifera extract was added to the metal solution mixture and stirred for 30 minutes at 600 rpm. Simultaneously, 3 gr of NaOH was dissolved in 50 mL of distilled water and heated at 80°C to form a basic solution. The metal solution was then slowly dripped into the NaOH solution while continuously stirring at 600 rpm for 60 minutes at 80°C until a black precipitate of $CoFe_2O_4$ formed. The precipitate was washed repeatedly with distilled water until the pH was neutral, then dried at 80°C for 7 hours and calcined at 600°C for 5,5 hours to produce $CoFe_2O_4$ powder with high crystallinity.

Meanwhile, Cdots were synthesized using a watermelon rind-based hydrothermal method. A total of 15 mL of grated watermelon rind was mixed with 15 mL of distilled water and 15 mL of ethanol, then stirred for 30 minutes until the solution was homogeneous. The mixture was put into a hydrothermal autoclave and heated at 180 °C for 3 hours. After cooling to room temperature, the reaction product was filtered with Whatman paper and the filtrate obtained was a Cdot solution. The fabrication process of $CoFe_2O_4$/Cdots nanocomposite was carried out by mixing 0,5 gr of $CoFe_2O_4$ powder into 20 mL of Cdot solution, then sonicated for 30 minutes to obtain a homogeneous dispersion. The suspension was then left for 24 hours at room temperature for the aging process, washed with distilled water until the pH was neutral, and dried at 90 °C for 4 hours to produce $CoFe_2O_4$/Cdot nanocomposite powder that was ready for characterization and photocatalytic testing. The overall synthesis process demonstrates the advantages of *green chemistry*, where natural plant extracts act as eco-friendly reducing and stabilizing agents without the use of hazardous chemicals. Biomolecules such as flavonoids, phenolics, and polysaccharides in *Moringa oleifera* extract play an essential role in controlling nucleation, limiting the growth of nanoparticles, and preventing agglomeration.

(a)

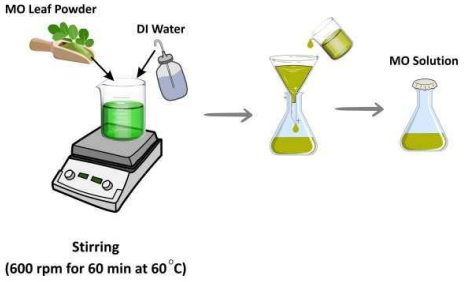

(b)

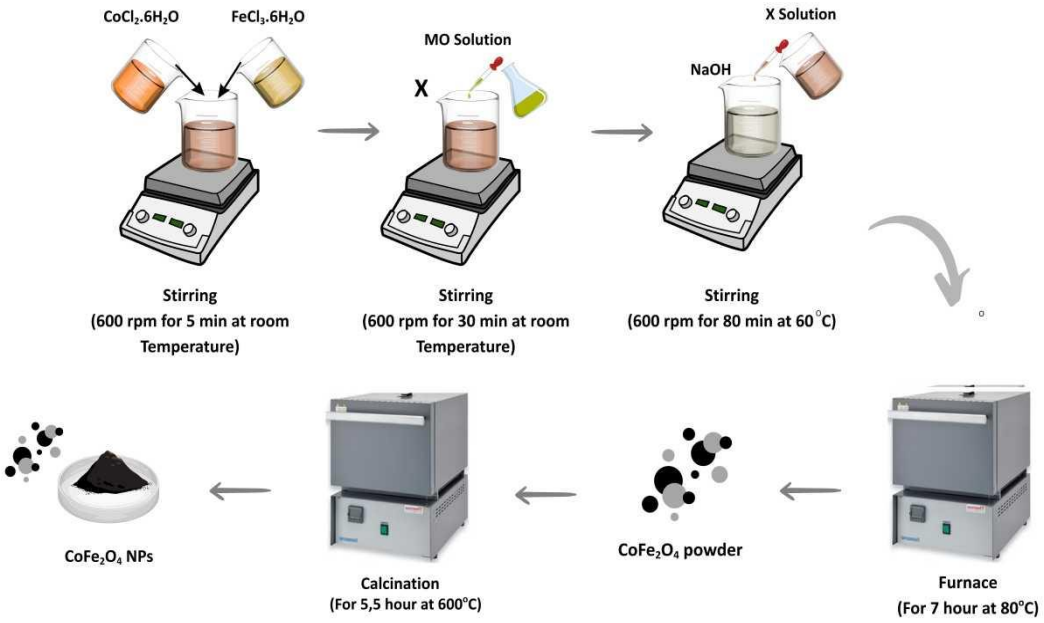

(c)

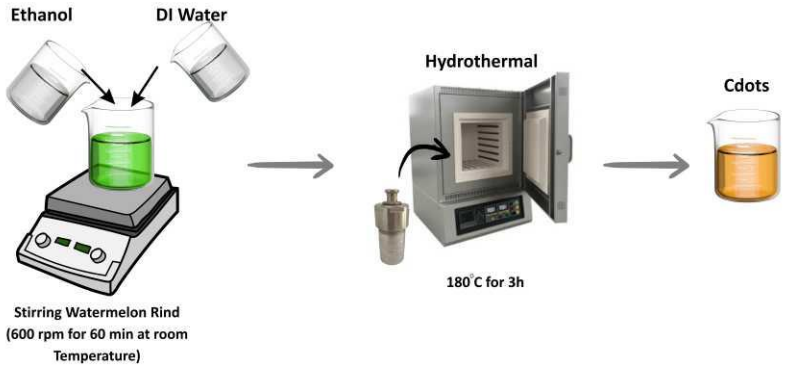

(d)

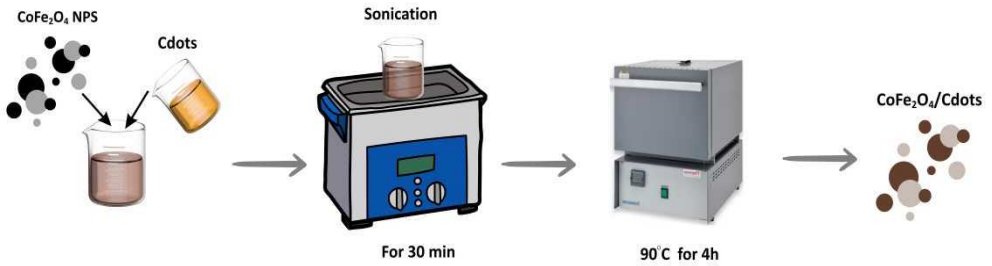

Figure 1. A schematic illustration shows the sequential synthesis steps of $CoFe_2O_4$/Cdots nanocomposites: (a) preparation of MO extract solution, (b) green synthesis of $CoFe_2O_4$ nanoparticles via the co-precipitation technique, (c) hydrothermal production of Cdots derived from watermelon rind waste, and (d) formation of $CoFe_2O_4$/Cdots nanocomposites through the self-assembly of Cdots onto the $CoFe_2O_4$ nanoparticle surface.

Characterization

Material characterization was carried out to determine the crystal structure, magnetic properties, and optical properties of the $CoFe_2O_4$/Cdots nanocomposite. X-ray diffraction (XRD) analysis was used to identify the crystal phase and determine the crystal lattice parameters of the $CoFe_2O_4$ cubic spinel system. The crystallite size was calculated using the Scherrer equation:

$$D = \frac{K\lambda}{\beta \cos\theta} \quad (1)$$

Note:
D = Crystallite size (nm),
K = The Scherrer constant (0.9)
λ = X-ray wavelength (0.15406 nm),
β = Peak Width at Half Maximum (FWHM) in radians
θ = Bragg angle.

In addition, the lattice parameter a is calculated using the geometric formula of the cubic spinel structure as follows:

$$a = d\sqrt{h^2 + k^2 + l^2} \quad (2)$$

Note:
a = the lattice parameter (Å)
d = the distance between crystal planes (Å) obtained from XRD data
h, k, and l = The Miller indices of the main diffraction planes.

The magnetic properties of the material were analyzed using a Vibrating Sample Magnetometer (VSM) to obtain a magnetic hysteresis curve and determine the saturation magnetization (Ms), coercivity (Hc), and remanence (Mr) values. A high Ms value indicates the catalyst's separation capability with an external magnetic field.

Optical analysis was carried out using a UV-Vis Spectrophotometer to determine the band gap energy (Eg) value using the Tauc plot method, which is expressed by the equation:

$$(\alpha h\nu)^n = A(h\nu - E_g) \quad (3)$$

Note:
α = The absorption coefficient (calculated from the absorbance)
$h\nu$ = The photon energy,
A = The constant, and
N = Depends on the type of electronic transition.
The value of Eg is obtained by extrapolating the graph of $(\alpha h\nu)^n$ against $h\nu$ until it intersects the energy axis.

Photocatalytic Test with Initial Adsorption Mechanism

Photocatalytic testing was conducted to evaluate the ability of the $CoFe_2O_4$/Cdots nanocomposite to degrade Methylene Blue (MB) dye. A 7 ppm MB stock solution was prepared by dissolving 0.0035 g of MB powder in 500 mL of distilled water. Fifty mL of the MB solution was taken and mixed with varying catalyst masses of 0.03 g, 0.05 gr, 0.07 g and 0.09 g, respectively. The mixture was stirred at 600 rpm in the dark for 20 minutes to reach initial adsorption equilibrium. After the adsorption process was complete, 250 µL of H_2O_2 was added, and the mixture was irradiated with three 10 W Philips UV lamps for 120 minutes. Samples were taken every 20 minutes, and the absorbance of the solution was measured at a wavelength of 664 nm using a UV-Vis spectrophotometer. The degradation efficiency of Methylene Blue was calculated using the equation:

$$Deg(\%) = \frac{C_0 - C_t}{C_0} \times 100\% \quad (4)$$

Note:
C_0 = The initial concentration of MB (after adsorption)
C_t = The concentration of MB at time *t*.

3. Result and Discussion

X-Ray Diffraction (XRD) Analysis

The crystalline structure of $CoFe_2O_4$ and $CoFe_2O_4$/Cdots composites synthesized via the green synthesis route was investigated using XRD. This characterization technique provides comprehensive information about the crystalline phase, lattice parameter, and structural quality of the synthesized materials. The recorded XRD patterns, as shown in Figure 2, were indexed to the standard reference from the Crystallography Open Database (COD No. 5910063), confirming that the dominant crystalline phase corresponds to $CoFe_2O_4$ with a cubic spinel structure. The most intense diffraction peak appeared at the (311) plane ($2\theta \approx 35.6°$), which is characteristic of spinel-type $CoFe_2O_4$, consistent with previously reported data (Jabbar et al., 2020).

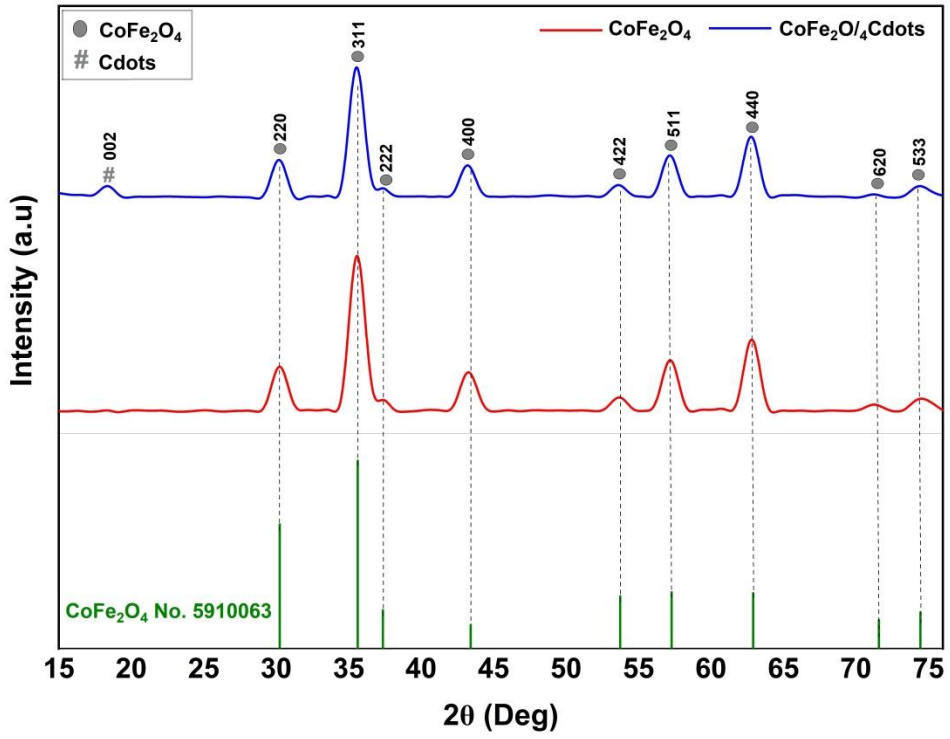

Figure 2. X-ray diffraction patterns of $CoFe_2O_4$ and $CoFe_2O_4$/Cdot

The XRD patterns of both $CoFe_2O_4$ and $CoFe_2O_4$/Cdots exhibit well-defined diffraction peaks at 2θ positions corresponding to the (220), (311), (222), (400), (422), (511), (440), (620), and (533) planes, which are the typical reflections of the cubic spinel ferrite structure. The sharpness and intensity of these peaks suggest high crystallinity of the synthesized nanoparticles. No secondary or impurity phases were detected, indicating that the synthesis process successfully yielded a single phase spinel $CoFe_2O_4$ structure with high phase purity. For the $CoFe_2O_4$/Cdots composite, the diffraction pattern remains consistent with that of pure $CoFe_2O_4$, suggesting that the incorporation of Cdots does not disturb the primary spinel lattice. However, a slight broadening and minor shift of peaks toward higher 2θ values were observed, which could be attributed

to microstrain within the lattice or the influence of Cdots at the particle surface. Additionally, a weak and broad peak around $2\theta \approx 18°$ was observed in the composite sample, corresponding to the amorphous carbon structure of Cdots (Pal et al., 2020). This observation confirms the successful integration of Cdots onto the surface of $CoFe_2O_4$ nanoparticles without altering the fundamental spinel framework.

Table 1. Crystallite size and lattice parameters of $CoFe_2O_4$ and $CoFe_2O_4$/Cdot

Sample	Crystallite (nm)	Lattice Parameter (Å)
$CoFe_2O_4$	5.8 ± 0.4	8,2 ± 0.2
$CoFe_2O_4$/Cdot	6.0 ± 0.2	8,3 ± 0.3

The average crystallite size of the samples was estimated using the Scherrer equation, while the lattice parameter was calculated using Bragg's law. The results, summarized in Table 1, reveal that the crystallite size of pure $CoFe_2O_4$ is approximately 5.8 ± 0.4 nm, which slightly increases to 6.0 ± 0.2 nm after Cdots incorporation. This small change indicates that Cdots may influence the crystal growth kinetics during the synthesis, leading to marginal enlargement of the nanocrystallites. The lattice parameter also exhibits a minor expansion from 8.32 ± 0.2 Å to 8.3 ± 0.3 Å, implying lattice strain induced by Cdots interaction or surface modification effects. Overall, the XRD analysis confirms the formation of a highly crystalline cubic spinel $CoFe_2O_4$ structure and demonstrates that the addition of Cdots does not disrupt the structural integrity of $CoFe_2O_4$. The slight lattice expansion and peak broadening observed suggest a successful surface modification by Cdots, which may enhance interfacial charge transfer and improve the optical or photocatalytic properties of the composite material.

Magnetic Properties Analysis (VSM)

The magnetic characteristics of $CoFe_2O_4$ and $CoFe_2O_4$/Cdots composites synthesized via the green synthesis route were analyzed using a Vibrating Sample Magnetometer (VSM) at room temperature. The obtained hysteresis loops are presented in Figure 3, while the corresponding magnetic parameters, including coercivity (Hc), remanent magnetization (Mr), and saturation magnetization (Ms), are summarized in Table 2, which clearly illustrate the ferrimagnetic nature of both samples. The characteristic S-shaped curves confirm that $CoFe_2O_4$ exhibits typical ferrimagnetic behavior originating from the antiparallel alignment of magnetic moments at the tetrahedral (A) and octahedral (B) sites within the spinel lattice. As depicted, the saturation magnetization (Ms) values for pure $CoFe_2O_4$ and the $CoFe_2O_4$/Cdots composite show a slight decrease after Cdots incorporation.

Under the influence of Cdots incorporation, noticeable modifications in the magnetic behavior of $CoFe_2O_4$ were observed. The interaction between the magnetic $CoFe_2O_4$ nanoparticles and the nonmagnetic carbon matrix introduced subtle but significant changes in the magnetic parameters, reflecting alterations in surface structure, particle-particle interaction, and cation distribution within the spinel lattice. The introduction of Cdots during synthesis may lead to partial surface coverage or interfacial bonding with $CoFe_2O_4$ nanoparticles, which can disrupt the exchange interactions between magnetic ions at the A and B sites. This results in a weakening of magnetic coupling and a reduction in the effective magnetic moment per formula unit. Furthermore, the Cdots can induce local lattice strain and modify surface anisotropy, which alters the energy landscape for magnetization alignment. These effects collectively contribute to variations in magnetic properties such as Ms, Hc, and Mr.

Overall, the presence of Cdots influences both the intrinsic and extrinsic magnetic characteristics of $CoFe_2O_4$ by introducing surface spin disorder and modifying interfacial magnetic interactions. This structural and magnetic interplay highlights the crucial role of the carbon component in tailoring the final magnetic behavior of the composite material, paving the way for its application in multifunctional magnetic nanodevices, data storage, and environmental remediation.

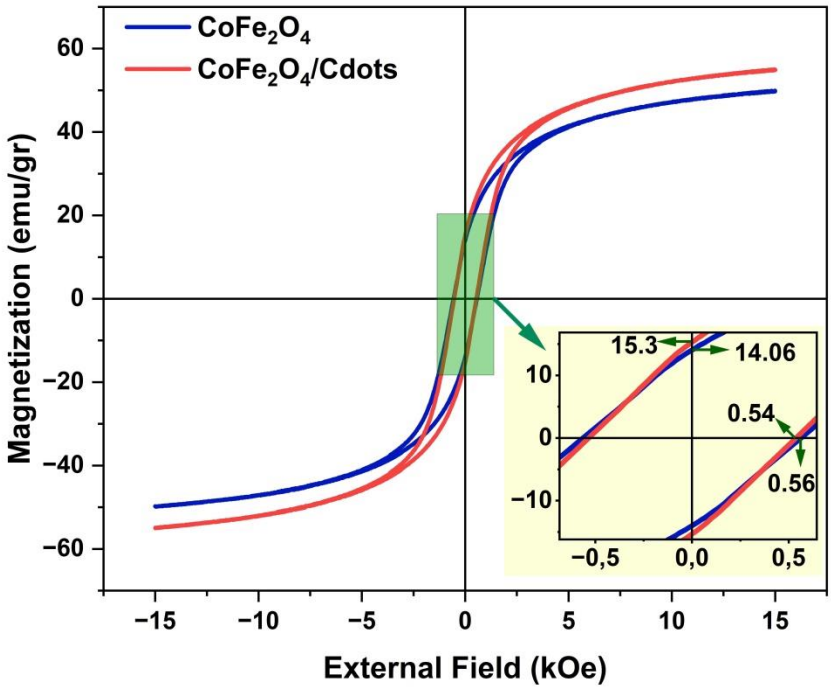

Figure 3. Hysteresis curves of $CoFe_2O_4$ and $CoFe_2O_4$/Cdots

As summarized in Table 2, The Ms value increased after the addition of Cdots, indicating that the interfacial interaction between $CoFe_2O_4$ and Cdots can strengthen the internal magnetic field of the composite material. The rise in Ms from 49.92 emu/g to 55.02 emu/g as summaryze in Table 2, suggests that the Cdots addition promotes better spin alignment at the surface and improves exchange interactions between magnetic ions within the spinel lattice. This enhancement may result from the strong coupling effect between the carbonaceous surface of Cdots and the Fe^{3+}-O^{2-}-Fe^{3+} and Co^{2+}-O^{2-}-Fe^{3+} linkages in $CoFe_2O_4$, which reduces spin disorder and magnetic frustration at the grain boundaries. Consequently, the magnetic moment per unit mass increases, contributing to improved magnetic performance. The observed decrease in Hc value from 563.73 Oe to 535.50 Oe confirms that $CoFe_2O_4$/Cdots exhibits softer magnetic behavior than pure $CoFe_2O_4$. A lower coercivity indicates that less energy is required to magnetize or demagnetize the composite, which is advantageous for materials that need to be magnetically recovered or recycled after catalytic use. The presence of Cdots may introduce nonmagnetic carbon layers at the particle surface, leading to reduced magnetic anisotropy and a decrease in domain wall pinning energy (Slimani et al., 2023).

Table 2. Coercivity, remanence and saturation values of $CoFe_2O_4$ and $CoFe_2O_4$/Cdots

Sampel	Hc (Oe)	Mr (emu/gr)	Ms (emu/gr)
$CoFe_2O_4$	563.73	14.03	49.92
$CoFe_2O_4$/Cdots	535.50	15.30	55.02

The increase in Mr value from 14.03 to 15.30 emu/g also supports the improved magnetic ordering of the nanocomposite. The higher remanent magnetization is associated with stronger dipole-dipole interactions and reduced surface spin canting. The presence of Cdots could act as a bridge that transfers electrons between Co and Fe ions, stabilizing the magnetic domains and improving magnetic coupling efficiency. Moreover, the particle size and crystallinity observed in the XRD results correlate with the magnetic parameters, where smaller crystallites tend to exhibit reduced coercivity and enhanced Ms due to increased surface spin mobility (Tatarchuk et al., 2017). From a practical standpoint, this magnetic behavior is highly beneficial for photocatalytic applications, as it enables easy recovery of the catalyst from aqueous media using an external magnetic field. The soft magnetic property ensures that the nanocomposite can be

repeatedly separated and reused without significant loss of activity, thereby enhancing the sustainability and cost-effectiveness of the process. Similar findings were reported by (Santiago et al., 2025), who observed that incorporating carbon-based nanostructures into ferrite systems improved both magnetic performance and recyclability. Overall, the combination of enhanced Ms, moderate Mr, and reduced Hc values confirms that the integration of Cdots effectively tailors the magnetic characteristics of $CoFe_2O_4$ toward an optimized soft ferromagnetic regime suitable for environmental remediation applications.

Overall, the VSM results confirm that both samples exhibit ferrimagnetic characteristics with narrow hysteresis loops, typical of soft magnetic materials. The slight decrease in magnetization and coercivity upon Cdots addition indicates surface modification effects and partial dilution of magnetic interactions. These changes suggest that the $CoFe_2O_4$/Cdots composite retains the essential magnetic features of cobalt ferrite while improving its magnetic responsiveness, an important factor for efficient electron transfer and photogenerated charge separation during photocatalytic processes.

Optical Properties Analysis

The optical properties of $CoFe_2O_4$ and $CoFe_2O_4$/Cdots composites were analyzed using UV-Visible (UV-Vis) spectroscopy to investigate the effect of Cdots incorporation on the electronic transition and light absorption characteristics of the material. This analysis is essential for understanding how the modification alters the optical band structure, which directly influences the photocatalytic efficiency of the composite. By examining the absorbance behavior across the wavelength range of 200-800 nm, the interaction between the semiconductor matrix ($CoFe_2O_4$) and the carbon-based modifier (Cdots) can be evaluated in terms of light harvesting capability and charge excitation potential. The resulting UV-Vis spectra are presented in Figure 4, showing distinct differences in absorption intensity and edge position between pure $CoFe_2O_4$ and the $CoFe_2O_4$/Cdots composite. Incorporation of Cdots into $CoFe_2O_4$ is expected to enhance photon absorption by introducing additional electronic states within the band structure, facilitating electron excitation under lower photon energy. These newly formed energy levels can reduce the effective band gap, thereby improving the utilization of visible light. Furthermore, the presence of Cdots may serve as an electron mediator, suppressing electron-hole

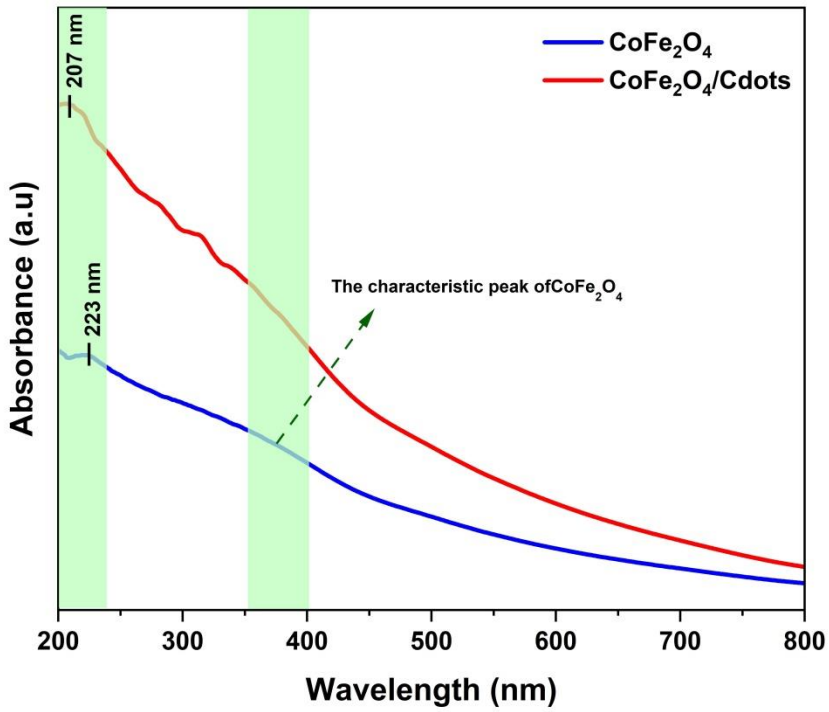

Figure 4. UV-Vis absorbance spectra of $CoFe_2O_4$ and $CoFe_2O_4$/Cdots

Figure 4 shows the UV-Vis absorbance spectra of $CoFe_2O_4$ and $CoFe_2O_4$/Cdots composites. Both samples exhibit strong absorption in the ultraviolet region, followed by a gradual decrease in intensity toward the visible range, which is characteristic of semiconducting materials. The absorption edge of $CoFe_2O_4$/Cdots appears at approximately 207 nm, slightly blue-shifted compared to pure $CoFe_2O_4$ at 223 nm, suggesting a modification in the electronic transition behavior due to the incorporation of Cdots. This blue shift is associated with an increase in the band gap energy, indicating that Cdots influence the charge distribution and quantum confinement effect within the composite structure. The modification of the optical edge demonstrates that the introduction of Cdots successfully alters the surface electronic structure of $CoFe_2O_4$ without changing its fundamental spinel phase.

Table 3. Absorbance peaks and optical band gap energy of $CoFe_2O_4$ and $CoFe_2O_4$/Cdots

Sample	Absorbance Peak (nm)	Band Gap (eV)
$CoFe_2O_4$	223	2.64
$CoFe_2O_4$/Cdot	207	3.15

The quantitative analysis of the optical properties is presented in Table 3, which summarizes the absorbance peaks and the corresponding optical band gap energies of $CoFe_2O_4$ and $CoFe_2O_4$/Cdots. Based on the Tauc relation plot, the values were calculated from the extrapolation of the linear portion of the Tauc plot as shown in Figure 5. The pure $CoFe_2O_4$ sample exhibits a band gap energy of 2.64 eV, while the $CoFe_2O_4$/Cdots composite shows a higher value of 3.15 eV, confirming the occurrence of a blue shift in the optical transition. The increase in band gap energy after Cdots incorporation indicates that the Cdots introduce localized surface states and improve electron confinement within the nanocomposite, resulting in higher excitation energy requirements.

Furthermore, the enhanced absorbance intensity of the $CoFe_2O_4$/Cdots composite compared to pure $CoFe_2O_4$ suggests that Cdots act as effective photosensitizers, improving light absorption and facilitating electron excitation from the valence band to the conduction band. The modification of optical behavior also implies a reduced recombination rate of photo generated charge carriers, which is beneficial for enhancing photocatalytic performance. Therefore, the integration of Cdots not only modifies the optical band gap but also improves the overall light-harvesting efficiency of $CoFe_2O_4$, making it a promising material for advanced photocatalytic and optoelectronic applications.

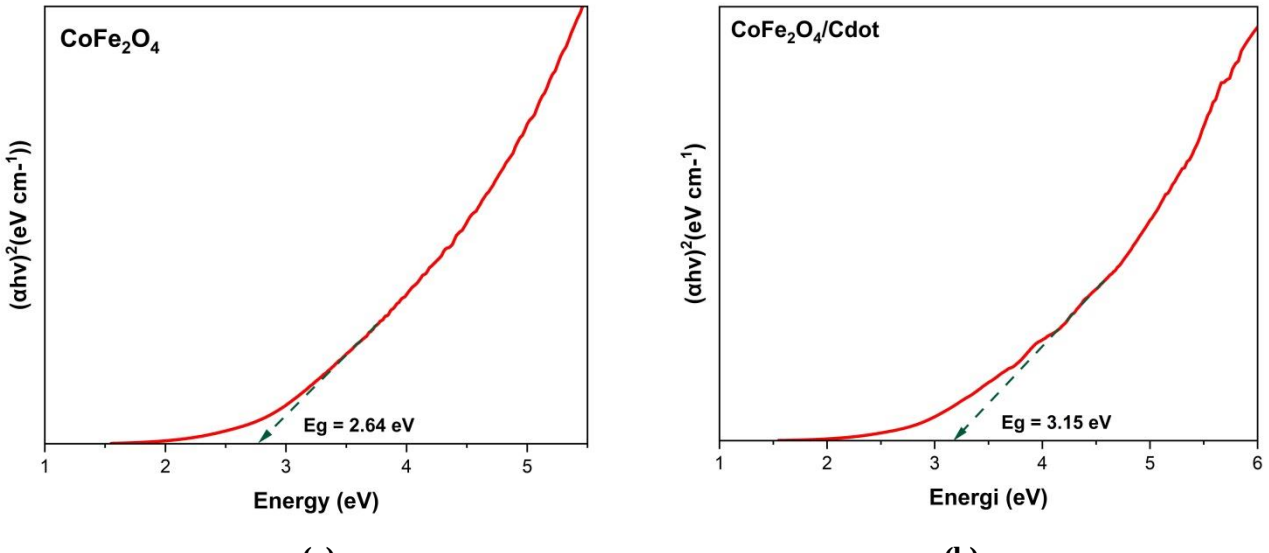

(a) **(b)**

Figure 5. Plot Tauc plot of (a) $CoFe_2O_4$ and (b) $CoFe_2O_4$/Cdots for band gap determination

Figure 5 show the Tauc plot derived from the absorbance data reveals that the optical band gap of $CoFe_2O_4$ after the addition of Cdots. This widening of the band gap corresponds to the observed blue shift and is commonly attributed to the *quantum confinement effect* and interfacial interaction between the ferrite matrix and the carbon nanoparticles. The Cdot acts as a surface modifier that introduces localized energy states, causing charge redistribution and slight distortion within the $CoFe_2O_4$ lattice. These interfacial effects modify the transition energy required for electron excitation, leading to the shift in optical response. The increase in band gap does not necessarily reduce photocatalytic efficiency; instead, it reflects an improved charge separation process. Cdots acts as an electron acceptor, trapping photoexcited electrons and suppressing recombination with holes in the $CoFe_2O_4$ matrix. This process prolongs the lifetime of charge carriers, thereby improving the generation of reactive radicals under UV illumination. In addition, oxygen-containing groups on the Cdot surface enhance the interaction between the composite and dye molecules through hydrogen bonding and π-π interactions, which promote effective adsorption and photodegradation. These findings confirm that the optical modification induced by Cdots incorporation not only alters the light absorption behavior but also optimizes the electronic band structure of $CoFe_2O_4$. The synergistic effects between both components contribute to better photoactivity, supporting the subsequent photocatalytic performance results. Similar optical tuning behavior due to carbon-based coupling has also been reported by (Anh et al., 2024), emphasizing that hybridization with Cdots is an effective route to improve both the optical and electronic properties of ferrite nanomaterials.

Photocatalytic Performance

The photocatalytic performance of the $CoFe_2O_4$/Cdots nanocomposites was investigated using MB as a model organic dye pollutant under ultraviolet (UV) light irradiation. The purpose of this evaluation was to determine the efficiency materials in degrading MB through photoinduced oxidation and reduction processes. The degradation reaction was tracked by recording the UV-Vis absorbance spectra of MB at different irradiation times, focusing on its main absorption peak at 664 nm. The gradual decrease in absorbance intensity indicates the decomposition of MB molecules into smaller fragments and mineralized products such as CO_2 and H_2O. The test was conducted under controlled conditions of dye concentration, catalyst dosage, and irradiation time to ensure reliable comparison between the two catalyst systems.

The UV-Vis absorbance spectra presented in Figure 6 display the photodegradation behavior of Methylene Blue for various $CoFe_2O_4$/Cdots catalyst masses. Initially, the MB solution shows a strong absorbance peak at 664 nm, characteristic of its chromophore group. As UV irradiation proceeds, the intensity of this peak progressively decreases, demonstrating the continuous degradation of MB molecules. The rate of absorbance decline is influenced by the amount of catalyst used. At lower catalyst loading (0.03 g), the degradation occurs more slowly due to the limited number of photoactive sites. With an increase in catalyst mass to 0.05 g and 0.07 g, the absorbance peak diminishes more rapidly, indicating higher photocatalytic activity. The most efficient performance is observed at 0.07 g, where nearly complete discoloration occurs after 120 minutes. However, further increasing the mass to 0.09 g causes a slight reduction in activity, likely due to particle agglomeration and decreased light penetration caused by scattering. This behavior confirms that there is an optimal catalyst dosage where the number of active sites and photon absorption are balanced.

The improved photocatalytic efficiency at moderate catalyst loading can be attributed to the enhanced generation of electron-hole pairs under UV illumination, which facilitates the formation of reactive radicals responsible for MB degradation. Excessive catalyst concentration, however, can lead to increased turbidity of the suspension, reducing photon availability and recombination of charge carriers. The presence of Cdots within the composite structure contributes to superior charge separation efficiency by acting as an electron reservoir, thus prolonging the lifetime of photogenerated carriers. Consequently, the $CoFe_2O_4$/Cdots composite demonstrates improved photoactivity compared to pure $CoFe_2O_4$, confirming the synergistic effect between the magnetic ferrite and carbon-based components. These findings strongly suggest that the optimization of catalyst mass is a critical factor for achieving maximum photocatalytic performance and efficient utilization of incident light energy.

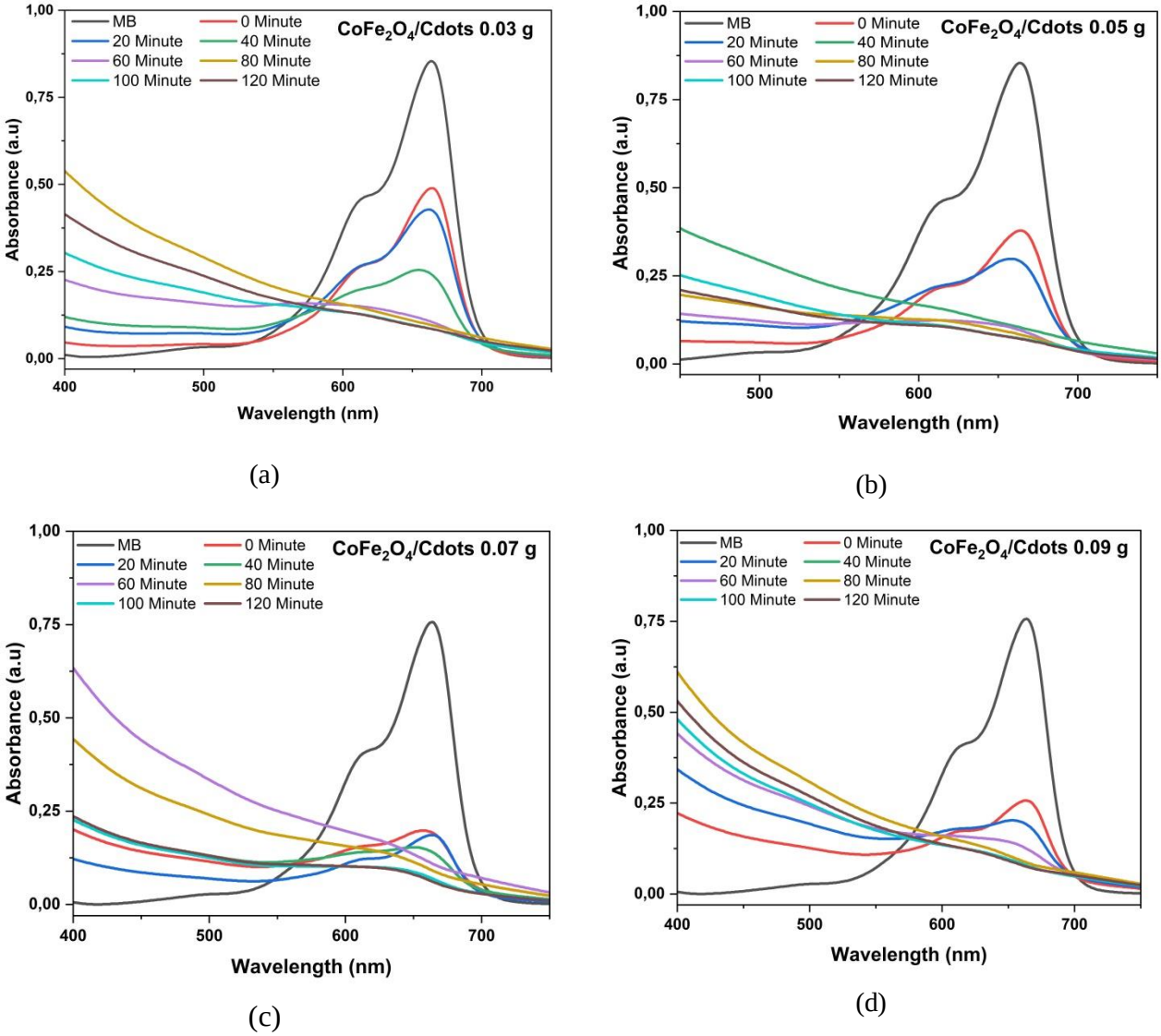

Figure 6. UV-Vis absorbance spectra of MB degradation using $CoFe_2O_4$/Cdots with different catalyst masses: (a) 0.03 g, (b) 0.05 g, (c) 0.07 g, and (d) 0.09 g.

The photocatalytic degradation efficiency was calculated based on the change in MB absorbance intensity with irradiation time. As shown in Figure 7, all $CoFe_2O_4$/Cdots catalyst masses exhibited a rapid decrease in MB concentration during the first 40 minutes, followed by a slower reaction rate approaching equilibrium at 120 minutes. The $CoFe_2O_4$/Cdots composite with 0.07 gr catalyst mass achieved the highest degradation efficiency of 91.9%, indicating optimal catalytic performance. The improved activity at this concentration is attributed to sufficient active sites for photon absorption and dye adsorption, as well as efficient charge separation across the $CoFe_2O_4$/Cdots interface. A comparison with previous research provides a clearer perspective on performance enhancement. According to (Puspitarum et al., 2022), pure $CoFe_2O_4$ nanoparticles achieved a maximum degradation efficiency of 60,8% under similar UV irradiation conditions for 120 minutes. In contrast, the $CoFe_2O_4$/Cdots nanocomposite synthesized in this study achieved a substantially higher degradation efficiency of 91.9% under the same duration. This difference of nearly 31,1 % highlights the significant role of Cdots incorporation in improving the photocatalytic performance of the ferrite matrix.

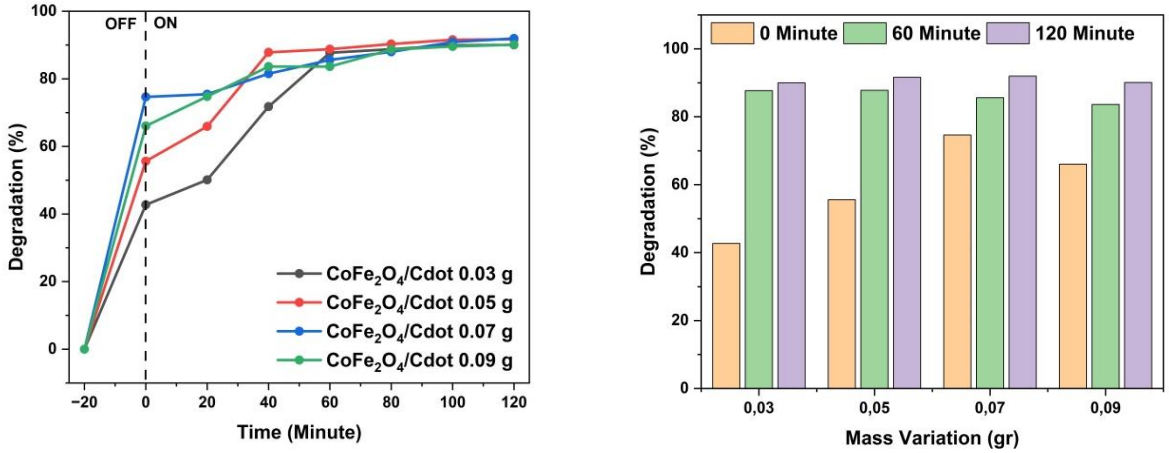

(a) (b)

Figure 7. Photocatalytic degradation efficiency of MB with (a) irradiation time and (b) different $CoFe_2O_4$/Cdots catalyst masses

Photocatalytic Mechanism with Initial Adsorption Stage

The photocatalytic degradation mechanism of Methylene Blue (MB) using $CoFe_2O_4$/Cdots nanocomposite can be described as a synergistic process involving an initial adsorption step, followed by photoexcitation, charge transfer, and oxidative degradation reactions. As illustrated in Figure 8, the first step is the adsorption of MB molecules onto the surface of the $CoFe_2O_4$/Cdots catalyst. This stage is crucial because it determines the availability of dye molecules at the catalyst interface where redox reactions occur. The abundant oxygen-containing functional groups on the surface of Cdots such as hydroxyl, carboxyl, and carbonyl enhance the adsorption of MB through hydrogen bonding and π–π* interactions. The high surface area of Cdots also facilitates the physical adsorption of MB molecules, ensuring close contact between the pollutant and the catalyst surface before photoreaction begins (Wang & Bin, 2019).

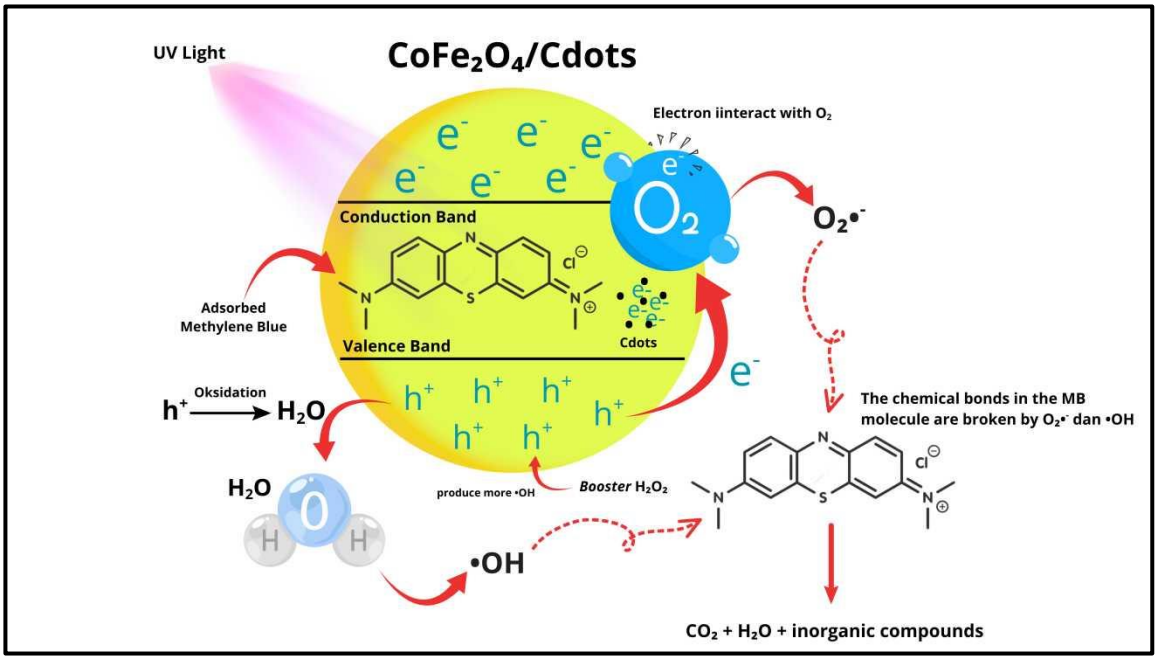

Figure 8. Proposed photocatalytic mechanism of Methylene Blue degradation by $CoFe_2O_4$/Cdot under UV irradiation

Upon UV light irradiation, the $CoFe_2O_4$/Cdots composite absorbs photons and generates electron-hole pairs (e^-/h^+). The electrons are excited from the valence band (VB) to the conduction band (CB) of $CoFe_2O_4$, leaving holes in the VB. The photogenerated electrons are quickly transferred to the Cdots, which acts as an electron acceptor and transport medium, effectively suppressing charge recombination. The accumulated electrons in Cdots subsequently react with dissolved oxygen molecules (O_2) to form superoxide radicals ($O_2{\cdot}^-$), while the holes in the VB of $CoFe_2O_4$ oxidize adsorbed water molecules to produce hydroxyl radicals (·OH). The reactive radicals generated in these processes are the main oxidative agents responsible for degrading MB molecules. The overall reactions can be summarized as follows:

$$MB + h\nu + O_2 + H_2O \xrightarrow{CoFe_2O_4/Cdots} CO_2 + H_2O + inorganic\ compounds \quad (4)$$

During this process, $O_2{\cdot}^-$ and ·OH radicals attack the chromophoric structures of MB, breaking the conjugated π-bond system and leading to decolorization and mineralization into CO_2, H_2O, and other inorganic ions. The reaction scheme shown in Figure 8 illustrates how these reactive oxygen species successively oxidize MB molecules into smaller intermediates before full decomposition. The role of Cdots is particularly important in enhancing this mechanism. It not only improves the initial adsorption of MB molecules but also serves as a bridge for rapid electron migration between $CoFe_2O_4$ and adsorbed oxygen species. This dual function significantly increases the lifetime of photogenerated charge carriers and promotes the continuous formation of oxidative radicals. Furthermore, the electron-rich nature of Cdots allows multiple cycles of charge exchange, sustaining the photocatalytic reaction for a longer duration. The initial adsorption mechanism plays a vital role in increasing the overall degradation efficiency. Without effective adsorption, many MB molecules remain in the bulk solution and fail to interact with the photoactive sites, thus lowering reaction kinetics (Ahmadian et al., 2017). The combination of strong adsorption capacity from Cdots and high photocatalytic reactivity from $CoFe_2O_4$ results in a highly efficient and recyclable system.

4. Conclusions

This study successfully demonstrated the synthesis and photocatalytic performance of green-synthesized $CoFe_2O_4$/Cdots nanocomposites prepared using *Moringa oleifera* extract and watermelon rind waste as sustainable precursors. The results revealed that the incorporation of Cdots into $CoFe_2O_4$ significantly enhanced its structural, optical, magnetic, and photocatalytic properties. Based on UV-Vis analysis, the $CoFe_2O_4$/Cdots nanocomposite exhibited a wider optical band gap of 3.15 eV compared to 2.64 eV for pure $CoFe_2O_4$, indicating improved light absorption and charge carrier mobility. The VSM analysis confirmed that the nanocomposite maintained soft magnetic behavior with higher saturation magnetization, enabling easy recovery and reuse of the catalyst.

Photocatalytic testing against Methylene Blue under UV irradiation showed that $CoFe_2O_4$/Cdot achieved a degradation efficiency of 91,9% at an optimum catalyst mass of 0.07 gr. This improvement is attributed to the synergistic effect between $CoFe_2O_4$ and Cdots, where Cdots act as both electron mediators and adsorption boosters, enhancing charge separation and promoting the generation of reactive oxygen species (·OH and $O_2{\cdot}^-$). The adsorption controlled mechanism plays a crucial role in this process, ensuring that dye molecules are effectively concentrated at the catalyst interface prior to photoactivation.

In general, the findings confirm that coupling ferrite materials with Cdots through a green synthesis route is an effective and environmentally friendly strategy to improve photocatalytic activity. The $CoFe_2O_4$/Cdots nanocomposite demonstrates great potential as a recyclable and efficient photocatalyst for wastewater treatment, particularly in the degradation of dye-based pollutants.

References

Ahmadian, S., Salavati-Niasari, M., & Safardoust-Hojaghan, H. (2017). Hydrothermal green synthesis and Ahmadian, S., Salavati-Niasari, M., & Safardoust-Hojaghan, H. (2017). Hydrothermal green synthesis and photocatalytic activity of magnetic CoFe2O4–carbon quantum dots nanocomposite by turmeric precursor. *Journal of Materials Science: Materials in Electronics*, *28*(21), 16205–16214. https://doi.org/10.1007/s10854-017-7522-1

Anh, V. C. N., Nhi, L. T. T., Dung, L. T. K., Hoa, D. T. N., Son, N. T., Uyen, N. T. T., Thu, N. N. U., Son, L. V. T., Hieu, L. T., Tuyen, T. N., & Khieu, D. Q. (2024). Photocatalytic degradation of methylene blue under visible light by cobalt ferrite nanoparticles/graphene quantum dots. *Beilstein Journal of Nanotechnology*, *15*, 475–489. https://doi.org/10.3762/BJNANO.15.43

Annamalai, A., Sangaraju, S., & Elumalai, S. (2025). Insights into carbon dots and conventional semiconductors hybrids: A trendsetter in photocatalytic hydrogen generation. *Coordination Chemistry Reviews*, *535*(February), 216646. https://doi.org/10.1016/j.ccr.2025.216646

Hannan, I. A., Eka Witrie, S., & Prasetya Adi, N. (2024). Dampak Pencemaran Air Akibat Limbah Industri Batik Printing di Kecamatan Pekalongan Utara Terhadap Kualitas Air Sungai. *Gudang Jurnal Multidisiplin Ilmu*, *2*(8), 34–42. https://gudangjurnal.com/index.php/gjmi/article/view/774

Hassaan, M. A., El-Nemr, M. A., Elkatory, M. R., Ragab, S., Niculescu, V. C., & El Nemr, A. (2023). Principles of Photocatalysts and Their Different Applications: A Review. In *Topics in Current Chemistry* (Vol. 381, Issue 6). Springer International Publishing. https://doi.org/10.1007/s41061-023-00444-7

Jabbar, R., Sabeh, S., & Hameed, A. (2020). Synthesis and Characterization of CoFe2O4Nanoparticles Prepared by Sol-GelMethod. *Engineering and Technology Journal*, *38*(2B), 47–53. https://doi.org/10.30684/etj.v38i2b.252

Kareem, H. A., Zaidi, M., Baqer, A. A., Hachim, S. K., ghazuan, T., Alasedi, K. K., Hameed, N. M., Aldulaim, A. K. O., Abid, M. K., Hussein, M. J., & Dahesh, S. M. A. (2022). Synthesis and Characterization of CoFe2 O4 Nanoparticles and Its Application in Removal of Reactive Violet 5 from Water. *Journal of Nanostructures*, *12*(3), 521–528. https://doi.org/10.22052/JNS.2022.03.005

Kunarti, E. S., Agustiningsih, D., Pambudi, F. I., Syoufian, A., & Santosa, S. J. (2025). Enhanced Photocatalytic Activity and Magnetic Properties of CoFe2O4/TiO2-Ag/S for Visible Light-Driven Photodegradation of Methylene Blue. *Indonesian Journal of Chemistry*, *25*(1), 232–243. https://doi.org/10.22146/ijc.100142

Lu, Y., Xu, L., Liu, C., & Zhang, Z. (2019). Synthesis and photocatalytic activity of composite magnetic photocatalyst Mn x Zn 1-x Fe 2 O 4 /α-Bi 2 O 3. *Materials Technology*, *34*(5), 301–311. https://doi.org/10.1080/10667857.2018.1554229

Lucas, M. S., Teixeira, A. R., Jorge, N., & Peres, J. A. (2025). *Industrial Wastewater Treatment by Coagulation – Flocculation and Advanced Oxidation Processes : A Review*.

Maddu, A., Meliafatmah, R., & Rustami, E. (2021). Enhancing photocatalytic degradation of methylene blue using zno/carbon dots nanocomposite derived from coffee grounds. *Polish Journal of Environmental Studies*, *30*(1), 273–282. https://doi.org/10.15244/pjoes/120156

Oladoye, P. O., Ajiboye, T. O., Omotola, E. O., & Oyewola, O. J. (2022). Methylene blue dye: Toxicity and potential elimination technology from wastewater. *Results in Engineering*, *16*(September), 100678. https://doi.org/10.1016/j.rineng.2022.100678

Pal, A., Sk, M. P., & Chattopadhyay, A. (2020). Recent advances in crystalline carbon dots for superior application potential. *Materials Advances*, *1*(4), 525–553. https://doi.org/10.1039/d0ma00108b

Puspitarum, D. L., Istiqomah, N. I., Tumbelaka, R. M., Kusumaatmaja, A., Oshima, D., Kato, T., & Suharyadi, E. (2022). High performance of magnetically separable and recyclable photocatalyst of green-synthesized CoFe2O4/TiO2 nanocomposites for degradation of methylene blue. *Advances in Natural Sciences: Nanoscience and Nanotechnology*, *13*(4), 45003. https://doi.org/10.1088/2043-6262/ac996b

Salehi, G., Bagherzadeh, M., Abazari, R., Hajilo, M., & Taherinia, D. (2024). Visible Light-Driven Photocatalytic Degradation of Methylene Blue Dye Using a Highly Efficient Mg-Al LDH@g-C3N4@Ag3PO4 Nanocomposite. *ACS Omega*, *9*(4), 4581–4593. https://doi.org/10.1021/acsomega.3c07326

Santiago, A. J., Palacios-Cabrera, C. B., Tecuapa-Flores, E. D., Bazany-Rodríguez, I. J., Narayanan, J., Padilla-Martínez, I. I., Aguilar, C. A., & Thangarasu, P. (2025). CO2 Adsorption by Carbon Quantum Dots/Metal Ferrites (M = Co2+, Ni2+, and Zn2+): Electrochemical and Theoretical Studies. *ACS Omega*, *10*(14), 13977–14000. https://doi.org/10.1021/acsomega.4c10723

Slimani, S., Talone, A., Abdolrahimi, M., Imperatori, P., Barucca, G., Fiorani, D., & Peddis, D. (2023). Morpho-Structural and Magnetic Properties of CoFe2O4/SiO2 Nanocomposites: The Effect of the

Molecular Coating. *The Journal of Physical Chemistry C*, *127*(18), 8840–8849. https://doi.org/10.1021/acs.jpcc.3c01252

Tatarchuk, T., Bououdina, M., Macyk, W., Shyichuk, O., Paliychuk, N., Yaremiy, I., Al-Najar, B., & Pacia, M. (2017). Structural, Optical, and Magnetic Properties of Zn-Doped CoFe2O4 Nanoparticles. *Nanoscale Research Letters*, *12*(1). https://doi.org/10.1186/s11671-017-1899-x

Vijayaram, S., Razafindralambo, H., Sun, Y. Z., Vasantharaj, S., Ghafarifarsani, H., Hoseinifar, S. H., & Raeeszadeh, M. (2024). Applications of Green Synthesized Metal Nanoparticles — a Review. *Biological Trace Element Research*, *202*(1), 360–386. https://doi.org/10.1007/s12011-023-03645-9

Wang & Bin. (2019). Carbon Dots/CoFe2O4 Mesoporous Nanosphere Composites As a Magnetically Separable Visible Light Photocatalyst. *Russian Journal of Physical Chemistry A*, *93*(2), 393–399. https://doi.org/10.1134/S0036024419020043